FEBS Letters 550 (2003) 168–174 FEBS 27565

Interdomain dynamics and ligand binding: molecular dynamics simulations of glutamine binding protein

Andrew Pang, Yalini Arinaminpathy, Mark S.P. Sansom, Philip C. Biggin*

Laboratory of Molecular Biophysics, Department of Biochemistry, The University of Oxford, South Parks Road, Oxford OX1 3QU, UK

Received 4 February 2003; revised 2 July 2003; accepted 22 July 2003

First published online 11 August 2003

Edited by Thomas L. James

Dedicated to the memory of Andrew Pang

Abstract Periplasmic binding proteins from Gram-negative bacteria possess a common architecture, comprised of two domains linked by a hinge region, a fold which they share with the neurotransmitter-binding domains of ionotropic glutamate receptors (GluRs). Glutamine-binding protein (GlnBP) is one such protein, whose crystal structure has been solved in both open and closed forms. Multi-nanosecond molecular dynamics simulations have been used to explore motions about the hinge region and how they are altered by ligand binding. Glutamine binding is seen to significantly reduce inter-domain motions about the hinge region. Essential dynamics analysis of inter-domain motion revealed the presence of both hinge-bending and twisting motions, as has been reported for a related sugar-binding protein. Significantly, the influence of the ligand on GlnBP dynamics is similar to that previously observed in simulations of rat glutamate receptor (GluR2) ligand-binding domain. The essential dynamics analysis of GlnBP also revealed a third class of motion which suggests a mechanism for signal transmission in GluRs.

Key words: Glutamine; Periplasmic binding protein; Essential dynamics; Molecular simulation

1. Introduction

It has long been recognised that ligand binding at domain interfaces may lead to significant changes in equilibrium conformation [1]. This has been suggested to play a role in e.g. initiation of signal transduction in neurotransmitter receptor and related proteins (see for example [2]). More recently, developments in molecular dynamics (MD) simulations [3] have enabled simulations to probe changes in interdomain dynamics coupled to ligand-induced changes in equilibrium conformation [4]. Such changes in dynamics may play a significant role in signal transmission within ligand-binding proteins. However, in order to test this hypothesis further, simulations are needed for a wider range of proteins than the relatively small number of neurotransmitter receptor domains for which X-ray structures are known. Fortunately, X-ray structures are known for a number of water-soluble ligand-binding proteins that share a common fold with neurotransmitter receptors. For example, a snail acetylcholine-binding protein [5] has a similar fold to the neurotransmitter-binding domain of the nicotinic acetylcholine receptor [6,7], and bacterial periplasmic binding proteins are homologous to the extracellular ligand-binding domain of rat and bacterial ionotropic glutamate receptors (GluRs) and *N*-methyl-D-aspartate receptors [8–11].

The cell envelope of Gram-negative bacteria, consisting of an outer membrane and an inner membrane in between which lies the periplasmic space, contains a number of complex transport systems [12,13]. To a first approximation, the outer membrane may be thought of as a passive molecular sieve. The inner membrane contains numerous active transporters for a wide range of low molecular weight compounds [14]. Periplasmic binding proteins are small (~250 residues) 'shuttle' proteins that carry low molecular weight ligands from the outer to the inner membrane. Upon ligand binding, periplasmic binding proteins change conformation such that they are subsequently recognised by a specific inner membrane transporter [15–17]. The X-ray structures of more than a dozen periplasmic binding proteins are known. These structures share a similar fold containing two distinct domains linked by a molecular hinge [1].

The structure of the glutamine-binding protein (GlnBP) from *Escherichia coli* is representative of the periplasmic binding proteins, and is closely related (and binds a similar ligand) to the comparable domains of mammalian and bacterial GluRs [18]. It is classified in the same SCOP [19] family (phosphate-binding protein-like) as human GluR2, but shares only 17% identity with the latter protein. In the GlnBP, binding of glutamine at a site between two domains causes a change in static equilibrium conformation corresponding to a closure of the two domains around the ligand (Fig. 1). By comparison with X-ray structures of sugar-binding proteins the closed form of the protein may also exist in the absence of ligand [20]. However, in the absence of ligand, it is thought that the open state(s) will predominate. Thus, it is suggested that both forms (and possibly intermediate states) are present in an equilibrium that is shifted towards the closed form upon ligand binding [21].

The crystal structures provide static snapshots of the two end-states of this equilibrium. To more fully understand the mechanism of ligand-induced conformational change one would also like to characterise the structural dynamics of the transition. In this paper we have used relatively long (~5 ns) MD simulations to compare the nature of motions about the inter-domain hinge in different states of GlnBP, revealing the dependence of the conformation dynamics on the presence or absence of bound ligand. Although a simulation time of ~5 ns is too short to observe repeated opening

*Corresponding author. Fax: (44)-1865-275182.
E-mail address: phil@biop.ox.ac.uk (P.C. Biggin).

0014-5793/03/$22.00 © 2003 Published by Elsevier B.V. on behalf of the Federation of European Biochemical Societies.
doi:10.1016/S0014-5793(03)00866-4

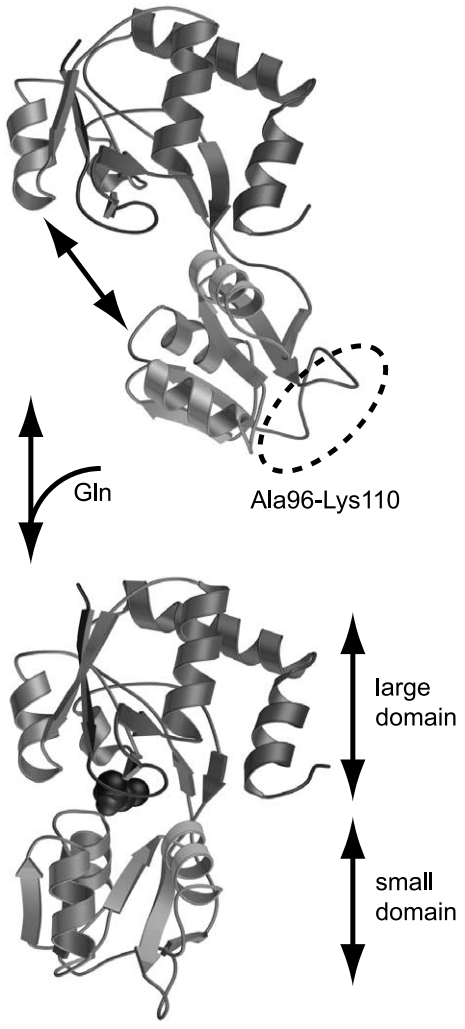

Fig. 1. The open (1GGG) and closed (1WDN) conformations of GlnBP as sampled by X-ray crystallographic studies. The proposed hinge-bending motion is indicated by the grey arrow, and bound glutamine is shown in spacefill. The location of a large dynamic loop (see text) between residues Ala96 and Lys110 is also indicated.

and closing of GlnBP the rate of closure of related periplasmic binding proteins has been estimated to be $\sim 2\times 10^8$ s^{-1} (i.e. equivalent to ~ 5 ns) [23]. Thus we might expect to observe at least some relevant aspects of GlnBP dynamics in 5 ns simulations. In particular, our simulations show that the hinge mechanism is more complex than one might at first assume, and suggest a possible conservation of structural dynamics that is relevant to the evolution of signal transduction in ligand-gated GluRs [2].

2. Materials and methods

Crystal structures are known for GlnBP with glutamine bound [21] (1WDN; closed conformation – see Fig. 1) and in an open apo form ([8] 1GGG). A closed apo state structure was generated by removing the bound glutamine from the ligand-bound structure (1WDN). To aid future comparisons all three co-ordinate sets were truncated to the shortest length protein (that of 1GGG) resulting in structures from Leu5 to Glu224. The N- and C-termini were acetylated and amidated respectively.

In preparation for MD simulations, each protein was placed in the centre of a box of approximate dimensions $80\times 80\times 80$ Å. Water molecules present within the X-ray structure were retained and c. 15 900 additional SPC [24] water molecules were added to fill the box. This yielded total system sizes of c. 50 000 atoms. All protein side chains were assumed to be in their default ionisation states based on pK_a calculations [25]. Sodium counterions were added to each simulation box to maintain electroneutrality.

All simulations were performed with GROMACS v3.0.3 [26]. Simulations were performed in the NPT ensemble, at a temperature of 300 K maintained using a Berendsen thermostat [27] with a coupling constant of 0.1 ps. Protein and water/ions were coupled independently. Pressure coupling used the Berendsen barostat with a coupling constant of 1.0 ps. Long-range electrostatic interactions were calculated using the particle mesh Ewald method [28] with a 10 Å cut-off. The LINCS algorithm [29] was used to restrain bond lengths. Each system was energy minimised followed by a short 200 ps simulation during which the protein, and if present ligand, non-hydrogen atoms were harmonically restrained with a force constant of 1000 kJ/mol/Å^2. All restraints were then removed and each simulation was run for 6 ns, saving co-ordinates and velocities every 5 ps for subsequent analysis. Typical CPU times on dual processor Intel Pentium III PCs running Linux kernel 2.4.18smp were 7 days per ns. As discussed below the first nanosecond of each simulation is treated as an equilibration period and for most of the analysis only the final 5 ns of simulation is considered.

Figures were rendered with Molscript [30], MOLMOL [31], Raster3D [32] and POV-ray [33].

3. Results and discussion

3.1. Molecular dynamics

An initial evaluation of structural drift is provided by analysis of the Cα atom root mean square deviations (RMSDs) from the initial structures as a function of time (Fig. 2A). Each simulation shows an initial jump (within c. 0.1 ns) of c. 1 Å (typical of such simulations and probably corresponding to small relaxation of the protein following release from its crystallographic environment), followed by longer length scale and time scale drift and/or fluctuations. It can be seen in Fig. 2A that for most of the time the RMSD for all three simulations is similar (between 2 and 5 ns) around 2 Å. Between 5 and 6 ns there are increases in fluctuations in all three simulations, though the apo seems to fluctuate slightly more. In contrast, the closed-ligand simulation exhibits smaller fluctuations. The peak fluctuations for all three simulations at 1 ns are similar in magnitude to those near the end of the simulation time. The trend in mobility from low (closed-ligand) to high (open-apo) can be visualised via examination of superimposed Cα traces (Fig. 2B).

Visual examination of the simulation trajectories alongside fitting structures on one domain and examining the time-dependent RMSD of the other domain suggested that one of the loops (Ala96 to Lys110, highlighted in Fig. 1) exhibited substantial motions. To quantify this further, we evaluated the root mean square fluctuation (RMSF) of each Cα as a function of residue number (Fig. 2C). (Note that for this and all subsequent analyses data were taken from the last 5 ns of each simulation, omitting the first nanosecond.) The results of the RMSF analysis indicated that in both the open-apo and the closed-apo conformations there were significant fluctuations centred around residues 96–110. In contrast, the ligand-bound form exhibited fluctuations around residues 18–24, 147–149 and 167–171. Both regions correspond to surface-exposed loops that have been postulated to play a role in receptor binding [21]. Conversely, there are three distinct regions where the open-apo and the closed-apo simulations both exhibit larger fluctuations than the closed-ligand simulation: the region around residue 10, residues 45–60 and residues 110–140.

These regions form the 'jaws' of the protein and furthermore contain the so-called doorkeeper residues thought to be important in maintaining access to the ligand-binding site [21]. In addition we analysed the secondary structure versus time (data not shown) and this was found to be stable throughout

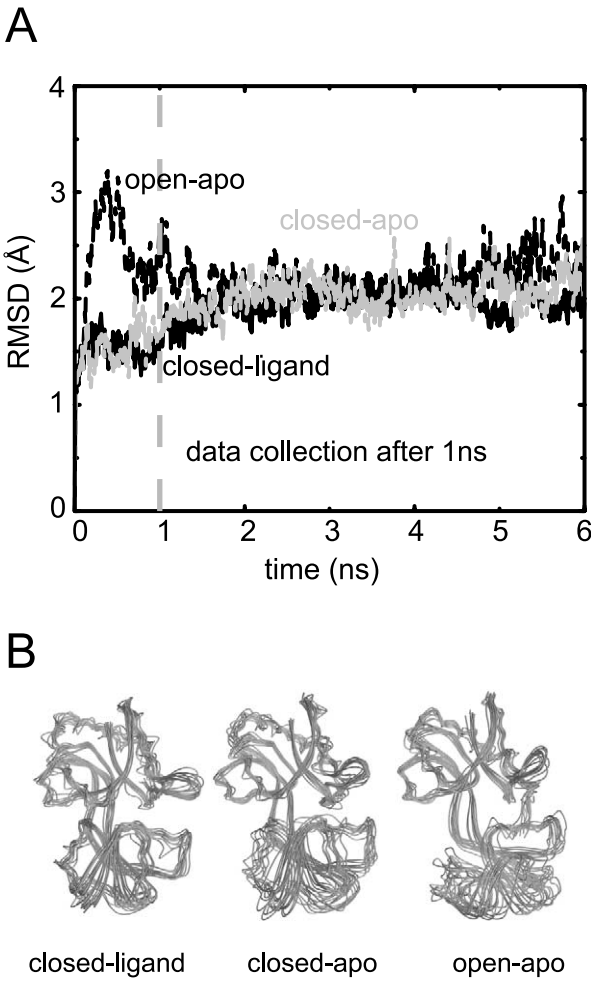

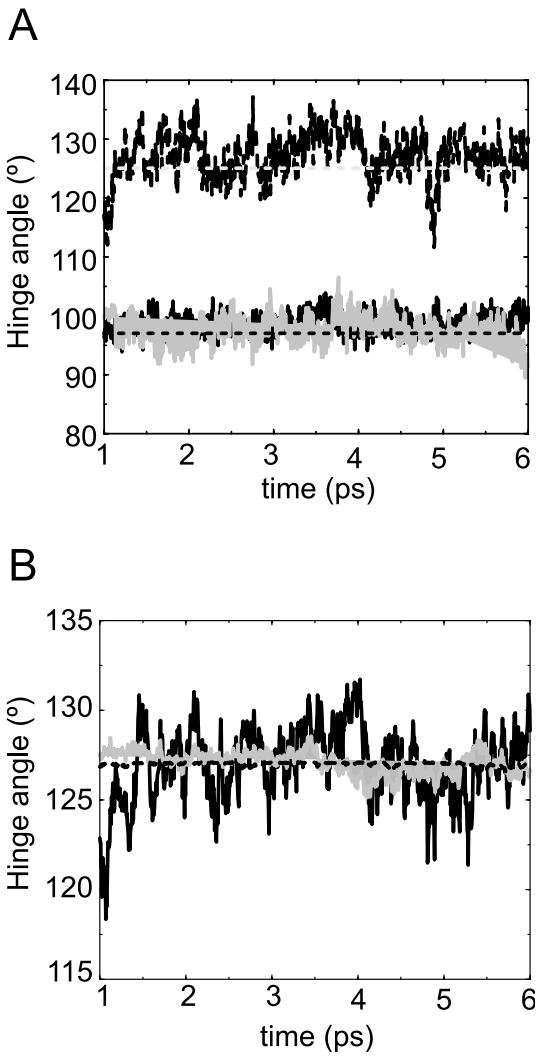

Fig. 3. A: Hinge-bending angle analysis of the three simulations. The hinge angle is defined as that formed by the centres of mass of the two domains and a central pivot point (defined as the centre of mass of the Cα atoms of Ser88 and Ala182). B: Hinge-bending analysis for the open-apo simulation from the trajectories filtered along the first three eigenvectors. Dashed black line is eigenvector 1, solid black line is eigenvector 2 and solid grey line is eigenvector 3.

←

Fig. 2. A: RMSD of the Cα atoms relative to the initial conformation for all three simulations: closed-ligand (solid black line), open-apo (dashed black line), closed-apo (solid grey line). B: Superimposed snapshots (every 0.5 ns from 1 to 6 ns) of the Cα traces for all three simulations. In each case, to highlight the nature of the motions, the superimposition of the structures has been on the upper (large) domain Cα atoms. C: RMSF for the closed-ligand (solid black line), open-apo (dashed black line) and closed-apo (solid grey line). The highly mobile loop between 97 and 106 is highlighted, as are residues at positions 22, 150 and 171 which have a noticeable increase in RMSF compared for the closed-ligand simulations compared to the apo simulations. Conversely, regions that possess a higher degree of fluctuation in the absence of ligand are also highlighted but specifically, the regions around residues 10, 45–60 and 110–140. Note that the 'doorkeeper residues' (Asp10 and Lys115) are contained within these regions.

the length of the simulation indicating that after the first nanosecond the majority of the motion appears to results from domain motion with respect to the other domain.

The principal conformational change proposed for the GlnBP and related periplasmic binding proteins is a simple hinge-bending motion [8,21]. Although one might not expect to fully sample such motions within a ~5 ns simulation, we did observe quite large motions in the open-apo simulation and so decided to examine the time dependence of hinge bending, calculated as the angle from the centre of mass of one domain to the suggested hinge residues (Ser88 and Ala182) to the centre of mass of the second domain. It is evident (Fig. 3) that the closed-apo and closed-ligand simulations exhibit not only a smaller mean hinge angle but also smaller hinge angle fluctuations than for the open-apo simulations. Comparison of the hinge angle standard deviations (3.9°, 2.4° and 1.7° respectively) suggests the order of the magnitude of movement is open-apo ≫ closed-apo > closed-ligand. The essential dynamics analysis (described below) revealed that most of the of hinge-bending motion can be ascribed to one particular eigenvector (the second one) as shown in Fig. 3B. Additional calculations of the inter-domain distance and radius of gyration versus time (not shown) gave similar plots.

3.2. Hydrogen bonding

In order to more fully characterise the differences in conformational dynamics we have examined the time-dependent patterns of hydrogen bonding in our simulations. During the closed-ligand simulation, the majority of hydrogen bonds reported in the crystal structure were maintained, and the overall number across the duration of the simulation was constant (with a mean value of 10). We also examined (see Fig. 4) the behaviour of three extra hydrogen bonds reported in the X-ray structure of the closed form (Tyr86:N–Gln184:$O^{\varepsilon 1}$; Lys87:N–Gln184:$O^{\varepsilon 1}$; and Ser88:O^{γ}–Tyr185:OH) which are suggested to confer rigidity on the hinge (see summary in Table 1). We did not observe a persistent Lys87:N–Gln84:$O^{\varepsilon 1}$ hydrogen bond in any of our simulations. Visual inspection suggested that this potential interaction corresponded to a distorted hydrogen bond geometry even in the crystal structures.

In the closed crystal structure, hydrogen bonding between the side chains of Lys115 and Asp10 is proposed to act as a 'doorkeeper' that locks the glutamine ligand into the binding pocket. Interestingly, residues 10 and 115 both lie in regions where there is a significant difference in dynamic fluctuations (as measured by Cα RMSFs – see Fig. 2C and above) between the apo and closed-ligand simulations. In the closed-ligand simulation, the Lys115–Asp10 hydrogen bonds are maintained, although dynamic swapping occurs between equivalent hydrogens on the Lys-N^{γ} and equivalent Asp-O^{δ} oxygens throughout the simulation. In contrast, in the closed-apo simulation, these hydrogen bonds were lost after approximately 1.5 ns and never reformed. This is a further indication of an enhanced degree of mobility in the closed-apo simulation.

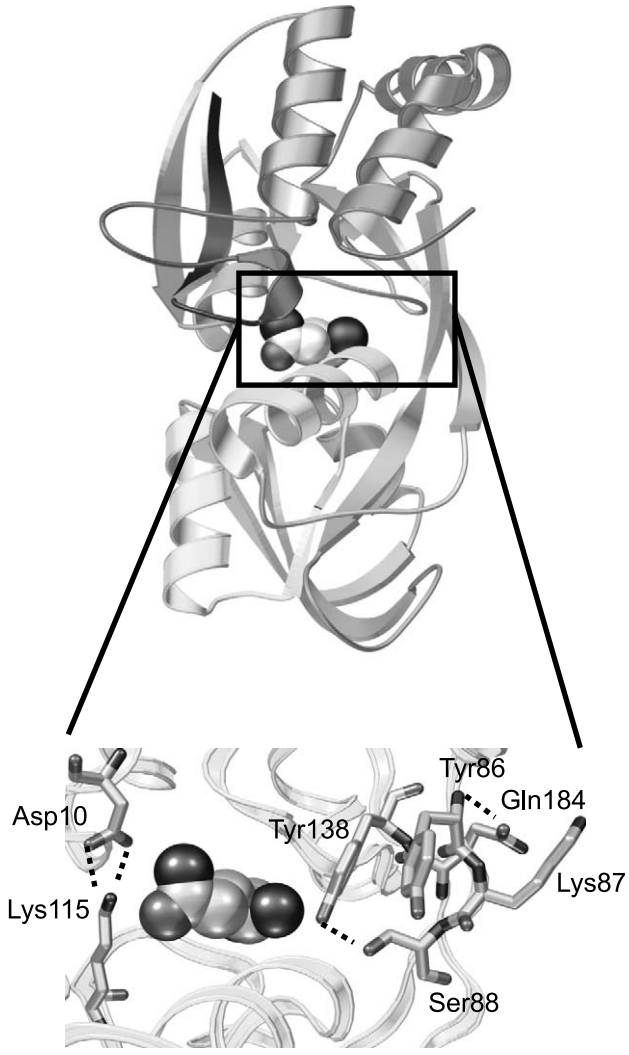

Fig. 4. Detailed picture of the binding site showing key hydrogen bonds from the hinge and the 'doorkeeper' (Asp10–Lys115). Glutamine is shown in spacefill representation.

3.3. Essential dynamics

The motions of a protein may be broken down into their principal components by essential dynamics analysis [34]. Applying such analysis to the Cα atom motions of the three simulations indicated that over 60% of these motions were accounted for by the first three eigenvectors. Recent application of such analysis to protein simulations [35,36] has suggested that analysis of the cosine content of the principal components provides an indicator of the extent of sampling. Examination of the open-apo simulation reveals that the co-

Table 1
Inter-domain hydrogen bonds

	Open-apo	Closed-ligand	Closed-apo
Tyr86:N–Gln184:$O^{\varepsilon 1}$	Not observed	Lost after ~3.5 ns	Maintained
Lys87:N–Gln184:$O^{\varepsilon 1}$	Not observed	Not observed	Not observed
Ser88:O^{γ}–Tyr185:OH	Gained after ~3.5 ns	Maintained	Lost after ~1 ns

A cut-off of 2.8 Å and 60° angle for the donor-H-acceptor was applied. All equivalent hydrogens were considered.

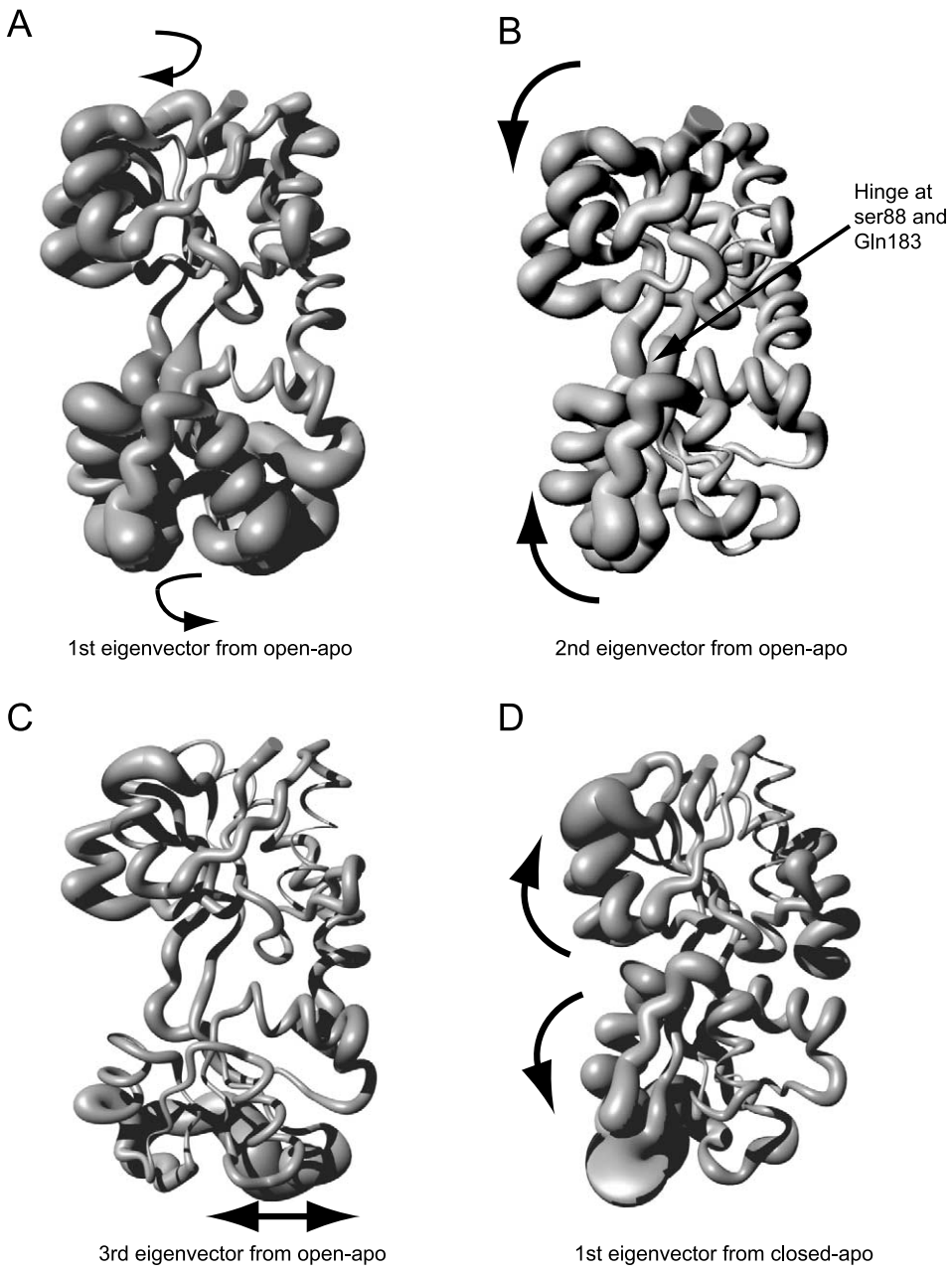

Fig. 5. Visual representation of the results of filtering of simulation trajectories along the principal eigenvectors allows visual inspection of the dominant motions. In each case the thickness of the sausage plot [31] indicates the extent of motion. Movements along the first three eigenvectors of the open-apo simulation are shown in A, B and C respectively. A: Movement along the first eigenvector can best be described as a twisting motion with the two lobes moving in parallel planes, as indicated by the grey arrows. B: Motion along the second eigenvector corresponds to a hinge-bending motion (arrows) about a hinge at Ser88 and Gln183. C: The third eigenvector corresponds to a large loop motion involving residues Ala96 to Lys110. In D a hinge-bending motion associated with the first eigenvector from the closed-apo simulation is shown. This should be compared with that depicted in B for the open-apo simulation.

sine content of eigenvectors 1, 2 and 3 was ~0.42, 0.14 and 0.11 indicating that the diffusive content of these eigenvectors was relatively low and thus they reveal genuine conformational transitions.

Filtering of the trajectories along each of the different eigenvectors allows visual inspection of the dominant motions for the open-apo simulation (Fig. 5A–C). Perhaps surprisingly, the motion associated with the first eigenvector can best be described as a twisting motion with the two lobes of the GlnBP moving in planes parallel to one another (Fig. 5A). Although such a twisting motion for a periplasmic binding protein has been suggested before [37], we did not expect this to form such a large contribution. The second eigenvector (Fig. 5B) corresponds more closely to a hinge-bending motion, enabling domain closure around the ligand. That this eigenvector corresponds to the hinge-bending motion is highlighted in Fig. 3B where the hinge angle is plotted as a function of time for trajectories filtered on the first three eigenvectors. The correlation coefficients of the hinge angle time series from the filtered trajectories with those from the 'raw' trajectory are 0.12, 0.55 and 0.16 for the first, second and third eigenvectors respectively. Thus it seems that the second eigen-

vector is responsible for the hinge bending. The pivot point in GlnBP for this motion is located at one end of the hinge region suggested by [21]. This differs from the reported hinge point in maltose-binding protein [37] and lysine/arginine/ornithine-binding protein (LAOBP) [38]. We located the hinge point for the second eigenvector motion using the program Hingefind [39]. Taking the two extreme projections along this eigenvector, the axis of the hinge runs through the residues Ser88 and Gln183 and the magnitude of the rotation is c. 30°. Applying Hingefind on the two crystal structures (i.e. open-apo vs. closed-ligand) gave a similar hinge location and a rotation of c. 57°. Thus the second eigenvector from the open-apo simulation reproduces quite well the conformational change suggested by the crystal structures.

The third eigenvector (Fig. 5C) corresponds to a movement primarily associated with the loop region located between residues Ala96 and Lys110. There is little indication of the importance for this region for GlnBP recognition by its target membrane transporter. However, we note with interest that this region maps onto the region of the glutamate receptor, GluR2, that is thought to be directly involved in the transmission of the binding signal to the transmembrane ion channel [40,41].

We also performed essential dynamics analysis on the closed-ligand and closed-apo simulations. The extent of the movements in these simulations is reduced compared to the open-apo simulation, making the assignment of distinct motions somewhat difficult. However, a hinge-bending motion could be assigned to the first eigenvector from the closed-apo simulation (Fig. 5D). Such a motion might be expected to dominate in the closed-apo simulation, leading eventually to a complete transition to the open-apo state.

4. Conclusions

In summary, we have shown that the extent of motion of GlnBP on a ~5 ns time scale is related primarily to the presence/absence of bound ligand and also, to a lesser extent, to the initial degree of domain closure. The open-apo simulation clearly exhibited significantly greater conformational fluctuation than the closed-apo simulation, which in turn showed a greater mobility than the closed-ligand system. This is in agreement with (albeit shorter) simulations of the structurally related ligand-binding domain of the rat GluR2 glutamate receptor [4]. The essential dynamics analysis revealed that a twisting motion and a hinge-bending motion are the dominant motions in the apo state of GlnBP. Hinge bending coupled with a twisting motion has also been suggested for the maltodextrin-binding protein [37] which shares the same fold. A further motion is associated with the loop region between Ala96 and Lys110. How this relates to recognition of GlnBP by its target membrane transporter remains uncertain, but it is interesting to note that LAOBP and the HisJ (histidine-binding) protein exhibit a high sequence similarity (~90%) in this region and share the same membrane transporter as one another [14]. The glutamine-binding protein has a distinct transporter associated with it and is not homologous to LAOBP in this region. Moreover, this region may be important for signal transmission in the ligand-binding domain of the ionotropic glutamate receptors [40,41].

Of course, we are aware that sampling of conformational change is incomplete in these simulations. There are a number of simulation approaches, including essential dynamics, by which this problem may be addressed [42]. For a number of ligand-binding proteins, one would like to predict the conformational changes from only one form of the protein. The results of the essential dynamics analysis for GlnBP suggest that simulations based on an open-apo structure may be more immediately productive in this respect. Such a simulation is likely to sample the closed conformation(s) if run for ~10 ns or more given the upper limits implied by the kinetic data [22]. If one could identify a tight-binding closed-ligand conformation (perhaps by ligand-docking approaches) then prediction of ligand-induced conformational transitions becomes feasible.

Acknowledgements: This work was supported by the Wellcome Trust and the BBSRC. We thank the Oxford Supercomputing Centre for computer time and Dr A. Grottesi for useful discussions.

References

[1] Gerstein, M., Lesk, A.M. and Chothia, C. (1994) Biochemistry 33, 6739–6749.
[2] Dingledine, R., Borges, K., Bowie, D. and Traynelis, S.F. (1999) Pharmacol. Rev. 51, 7–61.
[3] Karplus, M.J. and McCammon, J.A. (2002) Nat. Struct. Biol. 9, 646–652.
[4] Arinaminpathy, Y., Sansom, M.S.P. and Biggin, P.C. (2002) Biophys. J. 82, 676–683.
[5] Smit, A.B. et al. (2001) Nature 411, 261–268.
[6] Brejc, K., van Dijk, W.J., Klassen, R.V., Schuurmans, M., van der Oost, J., Smit, A.B. and Sixma, T.K. (2001) Nature 411, 269–276.
[7] Unwin, N. (2002) Novartis Found. Symp. 245, 5–15.
[8] Hsaio, C.-D., Sun, Y.-J., Rose, J. and Wang, B.-C. (1996) J. Mol. Biol. 262, 225–242.
[9] Armstrong, N., Sun, Y., Chen, G.-Q. and Gouaux, E. (1998) Nature 395, 913–917.
[10] Madden, D.R. (2002) Nat. Rev. Neurosci. 3, 91–101.
[11] Furukawa, H. and Gouaux, E. (2003) EMBO J. 22, 2873–2885.
[12] Buchanan, S.K. (2001) Trends Biochem. Sci. 1, 3–6.
[13] Ferguson, A.D. and Deisenhofer, J. (2002) Biochim. Biophys. Acta 1565, 318–332.
[14] Ames, G.F.-L. (1986) Annu. Rev. Biochem. 55, 397–425.
[15] Nohno, T., Saito, T. and Hong, J.-S. (1986) Mol. Gen. Genet. 205, 260–269.
[16] Boos, W. and Lucht, J.M. (1996) in: *Escherichia coli* and *Salmonella*: Cellular and Molecular Biology (Neidhardt, F.C. et al., Eds.), pp. 1175–1209, ASM Press, Washington, DC.
[17] Fukami-Kobayashi, K., Tateno, Y. and Nishikawa, K. (1999) J. Mol. Biol. 286, 279–290.
[18] Lampinen, M., Pentikäinen, O., Johnson, M.S. and Keinänen, K. (1998) EMBO J. 17, 4704–4711.
[19] Murzin, A.G., Brenner, S.E., Hubbard, T. and Chothia, C. (1995) J. Mol. Biol. 247, 536–540.
[20] Flocco, M.M. and Mowbray, S.L. (1994) J. Biol. Chem 268, 8931–8936.
[21] Sun, Y.-J., Rose, J., Wang, B.-C. and Hsiao, C.-D. (1998) J. Mol. Biol. 278, 219–229.
[22] Weiner, J.H. and Heppel, L.A. (1971) J. Biol. Chem. 246, 6933–6941.
[23] Miller III, D.M., Olson, J.S., Pflugrath, J.W. and Quicho, F.A. (1983) J. Biol. Chem 258, 13665–13672.
[24] Hermans, J., Berendsen, H.J.C., van Gunsteren, W.F. and Postma, J.P.M. (1984) Biopolymers 23, 1513–1518.
[25] Adcock, C., Smith, G.R. and Sansom, M.S.P. (1998) Biophys. J. 75, 1211–1222.
[26] Lindahl, E., Hess, B. and van der Spoel, D. (2001) J. Mol. Model. 7, 306–317.
[27] Berendsen, H.J.C., Postma, J.P.M., van Gunsteren, W.F., DiNola, A. and Haak, J.R. (1984) J. Chem. Phys. 81, 3684–3690.
[28] Darden, T., York, D. and Pedersen, L. (1993) J. Chem. Phys. 98, 10089–10092.

[29] Hess, B., Bekker, J., Berendsen, H.J.C. and Fraaije, J.G.E.M. (1997) J. Comp. Chem. 18, 1463–1472.
[30] Kraulis, P.J. (1991) J. Appl. Crystallogr. 24, 946–950.
[31] Koradi, R., Billeter, M. and Wüthrich, K. (1996) J. Mol. Graph. 14, 51–55.
[32] Merritt, E.A. and Bacon, J. (1997) Methods Enzymol. 277, 505–524.
[33] www.povray.org.
[34] Amadei, A., Linssen, A.B.M. and Berendsen, H.J.C. (1993) Proteins Struct. Func. Genet. 17, 412–425.
[35] Hess, B. (2000) Phys. Rev. E 62, 8438–8448.
[36] Hess, B. (2002) Phys. Rev. E 65, 0319101–03191010.
[37] Sharff, A.J., Rodseth, L.E., Spurlino, J.C. and Quicho, F.A. (1992) Biochemistry 31, 10657–10663.
[38] Oh, B.-H., Pandit, J., Kang, C.-H., Nikaido, K., Gokcen, S., Ames, G.F.-L. and Kim, S.-H. (1993) J. Biol. Chem. 268, 11348–11355.
[39] Wriggers, W. and Schulten, K. (1997) Proteins Struct. Funct. Genet. 29, 1–14.
[40] Armstrong, N. and Gouaux, E. (2000) Neuron 28, 165–181.
[41] Sun, Y., Olson, R., Horning, M., Armstrong, N., Mayer, M.L. and Gouaux, E. (2002) Nature 417, 245–253.
[42] Young, M.A., Gonfloni, S., Superti-Furga, G., Roux, B. and Kuriyan, J. (2001) Cell 105, 115–126.